

受入

79-12-106

高工研圖書室

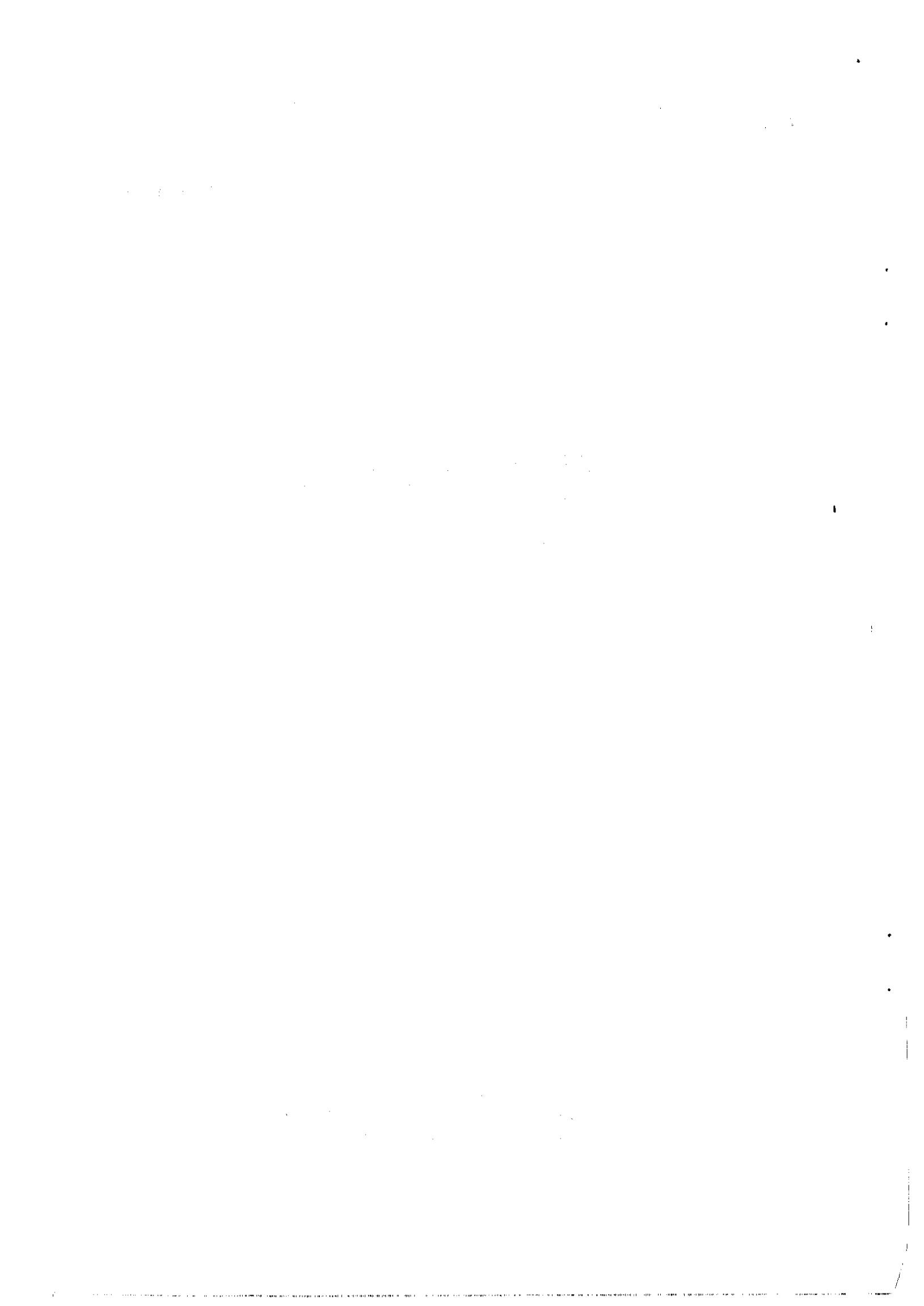
EUROPEAN ORGANIZATION FOR NUCLEAR RESEARCH

CERN-EP/79-118  
9 October 1979

DIRECT PRODUCTION OF SINGLE PHOTONS  
AT THE CERN INTERSECTING STORAGE RINGS

Athens-Athens-Brookhaven-CERN Collaboration

Presented at the  
EPS Int. Conf. on High Energy Physics  
Geneva, 27 June-4 July 1979



## DIRECT PRODUCTION OF SINGLE PHOTONS AT THE CERN INTERSECTING STORAGE RINGS

Athens-Athens-Brookhaven-CERN Collaboration

M. Diakonou, C. Kourkouvelis and L.K. Resvanis  
University of Athens, Athens, Greece.

T.A. Filippas, E. Fokitis and C. Trakkas  
National Technical University, Athens, Greece.

A.M. Cnops, J.H. Cobb<sup>1)</sup>, E.C. Fowler<sup>2)</sup>, D.M. Hood<sup>3)</sup>, S. Iwata<sup>4)</sup>,  
R.B. Palmer, D.C. Rahm, P. Rehak and I. Stumer  
Brookhaven National Laboratory<sup>5)</sup>, Upton, NY, USA.

C.W. Fabjan, T. Fields<sup>6)</sup>, D. Lissauer<sup>7)</sup>, I. Mannelli<sup>8)</sup>, W. Molzon,  
P. Mouzourakis, K. Nakamura<sup>9)</sup>, A. Nappi<sup>8)</sup> and W.J. Willis  
CERN, Geneva, Switzerland.

*(Presented by C.W. Fabjan)*

### ABSTRACT

Single-photon production in pp collisions at  $30 < \sqrt{s} < 62$  GeV has been measured with liquid-argon/lead calorimeters at the CERN ISR. This process, indicative of direct constituent interaction, remains approximately constant with increasing  $\sqrt{s}$ . For fixed  $\sqrt{s}$ , the single-photon to  $\pi^0$  ratio increases strongly with increase in  $p_T$ ;  $\gamma/\pi^0$  is  $0.25 \pm 0.08$  at  $5.0 < p_T < 6.5$  GeV/c for these interactions.

### 1. INTRODUCTION

Hadron-induced production of single photons has been investigated rather extensively in recent years, both experimentally and theoretically. Early interest in these studies was partly motivated by the conjecture<sup>1)</sup> that the level of direct  $\gamma$  production, and in particular its  $\sqrt{s}$  dependence, might discriminate in a sensitive way between different models of constituent scattering and therefore help in the understanding of large transverse momentum phenomena. At present, within the framework of QCD analyses, copious production of direct photons is one of the clearest predictions of this theory: provided this reaction is probed at large enough transverse momentum, the point-like coupling of the photon to the quarks should be at the origin of the dominant source for direct photons.

---

1) Now at Lancaster University, England.

2) Permanent address: Purdue University, W. Lafayette, Ind., USA.

3) Now at David Lipscomb College, Nashville, Tenn., USA.

4) Permanent address: Nagoya University, Nagoya, Japan.

5) Research supported under the auspices of the US Department of Energy.

6) Permanent address: Argonne National Laboratory, Argonne, Ill., USA.

7) Permanent address: Tel-Aviv University, Israel.

8) On leave of absence from the University of Pisa, and INFN, Sezione di Pisa, Italy.

9) Permanent address: University of Tokyo, Japan.

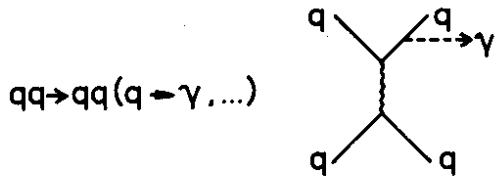


Fig. 1 Lowest-order QCD diagram for "final bremsstrahlung" of high  $p_T$  photons. There are also related processes of  $gq$ ,  $gg$ ,  $q\bar{q}$ , and  $g\bar{q}$  scattering.



Fig. 2 QCD diagrams contributing to "prompt" production of high- $p_T$  photons

Several theoretical groups have studied  $\gamma$  production within the framework of QCD<sup>2)</sup>. Some of the lowest-order diagrams are shown in Figs. 1 and 2. The physics indicates the consideration of two distinct classes of  $\gamma$  sources. As represented in Fig. 1, the photon may fragment in a bremsstrahlung-like process from the scattered quark and be observed together with the other quark fragments in a jet. Dominating however, and very different in the structure of the final state, are subprocesses where the photon participates directly in the scattering. Two diagrams for such "prompt" processes are shown in Fig. 2. For the reaction

$$q\bar{q} \rightarrow \gamma g$$

the corresponding invariant cross-section is found to be

$$E \frac{d\sigma}{d^3p} (pp \rightarrow \gamma) = C \left[ f_q(x), f_{\bar{q}}(x) \right] \frac{(1 - x_T)^{11}}{p_T^4},$$

where  $C [f_q(x), f_{\bar{q}}(x)]$  contains the dependence on the quark and antiquark distribution functions. In  $pp$  collisions, the dominant subprocess is, however, the gluon equivalent of Compton scattering:

$$gq \rightarrow \gamma q,$$

for which the  $pp$  production cross-section is calculated to be

$$E \frac{d\sigma}{d^3p} (pp \rightarrow \gamma) = C' \left[ f_q(x), f_g(x) \right] \frac{(1 - x_T)^6}{p_T^4}.$$

Should this description be valid, one would expect to observe events with a most striking signature: a high- $p_T$  photon, unaccompanied by other particles, recoils against a high-multiplicity jet of hadrons. Moreover, in the kinematical region where this reaction dominates, single-photon production provides a probe of the gluon distribution function: these single-photon studies of the gluon distributions are analogous to quark distribution studies in deep-inelastic lepton-nucleon scattering.

## 2. EXPERIMENTAL APPROACHES

Different experimental approaches are summarized in Table 1.

Table 1  
Experimental approaches

Measurement	Technique	Comments
Low-mass, high- $p_T$ virtual $\gamma$	e pairs from internal conversion	Very clean signature, reduced sensitivity
High- $p_T$ , real $\gamma$	Identification of photons and discrimination against $\pi^0$ 's	Good sensitivity, devastating background
	Measurement of conversion probability in external converter	Statistical method

The method of slightly virtual photons (low mass, large transverse momentum) is characterized by the experimentally very clean signature of electron pairs resulting from internal conversion, albeit with greatly reduced sensitivity. Alternatively, real high- $p_T$  photons may be identified by appropriate experimental techniques. The method offers good sensitivity provided that the devastating background from trivial sources, such as  $\pi^0$  and  $\eta$  decay, can be treated experimentally. In a variation of this identification method, the conversion probability into  $e^+e^-$  pairs of neutral electromagnetic clusters is measured in an appropriately chosen external converter. Hence one determines the average number of photons per cluster and may evaluate the level of the direct one-photon contribution. This is a statistical method and does not allow event-by-event identification of possible direct photons.

All three techniques have provided results, which will be discussed in the following section.

## 3. RESULTS

### 3.1 Virtual photon measurements

Results on low-mass, high- $p_T$  electron pairs and their implication on the level of direct  $\gamma$  production were published some time ago<sup>3)</sup>. The mass range chosen was

$$200 \text{ MeV} < m_{ee} < 600 \text{ MeV} .$$

A comparison with the simultaneously measured inclusive  $\rho$  production,  $pp \rightarrow \rho(\rho \rightarrow e^+e^-) + X$ , allowed a sensitive check of systematic experimental effects. The experiment was rate-limited for  $p_T \gtrsim 3 \text{ GeV}/c$ .

The measured production of electron pairs from virtual photons implies an expected level of direct photon production<sup>4)</sup>:

$$(q^2 + m^2)^{1/2} \frac{d\sigma(\gamma + ee)}{d^3q dm^2} = \frac{\alpha}{2\pi m^2} R \left( \frac{\gamma}{\pi^0} \right) \left[ E \frac{d\sigma(\pi^0)}{d^3p} \right] ,$$

where we have assumed  $m_T$  scaling and evaluated the invariant  $\pi^0$  cross-section for given  $q$  and  $m^2$  by the relations  $p_L = q_L$  and  $p_T^2 = q_T^2 + m^2$ . The ratio  $R(\gamma/\pi^0)$  of direct photon to  $\pi^0$  production is expected to have a small  $p_T$  dependence, evaluated to be between a constant and  $p_T^2$  in most models, and is not very significant over the small  $p_T$  range covered by the experiment. This measurement found as an upper limit for direct  $\gamma$  production

$$R\left(\frac{\gamma}{\pi^0}\right) = (0.55 \pm 0.92)\% \quad \text{for} \quad 2.0 \leq p_T \leq 3.0 \text{ GeV}/c.$$

Later, a similar result was obtained by another group working at the ISR<sup>5</sup>).

### 3.2: Real photon measurements

The characteristics of the A<sup>2</sup>BC apparatus that are relevant for the single-photon programme are summarized in Table 2. The apparatus consists essentially of up to four large-solid-angle electromagnetic shower detectors<sup>6</sup>). The modularity permitted several different experimental layouts (Fig. 3) and, as a consequence, control of some important systematic

Table 2

A<sup>2</sup>BC  $\gamma$  work: relevant apparatus aspects

Features	Parameters	Consequences
Modular, electromagnetic shower detector	4	Vary layout (and some systematics)
Large area	$65 \times 170 \text{ cm}^2/\text{module}$	
Highly segmented	Transv. $\sim 2 \times 140 \text{ cm}^2$ 4-fold longitudinal read-out	$\delta x \approx 5 \text{ mm}$ $\gamma/\text{hadron}$ discrimination in trigger and off-line
Liquid-argon ion chamber technique	Photon with $E_\gamma \gtrsim 300 \text{ MeV}$ identified	Stability and reproducibility of operating conditions

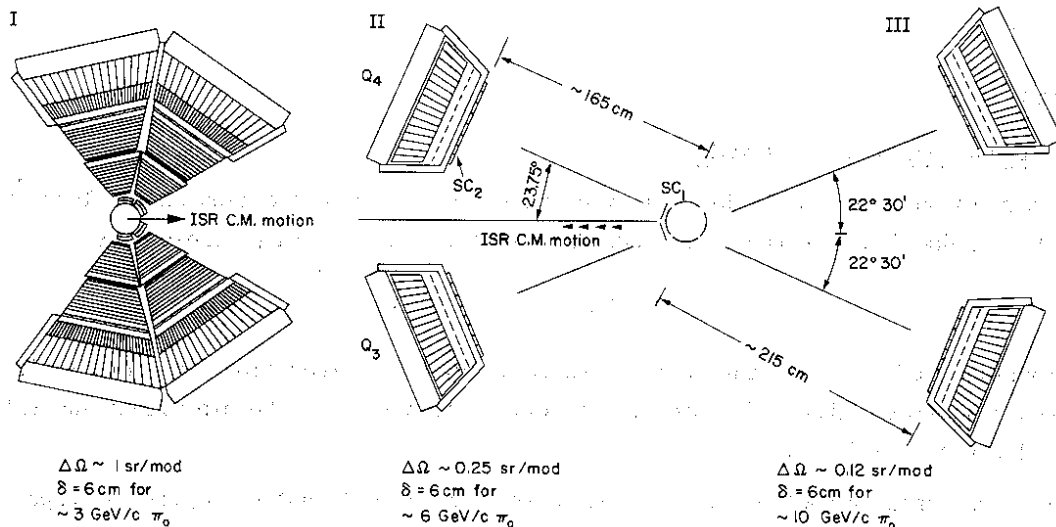


Fig. 3 The apparatus of the A<sup>2</sup>BC Collaboration showing schematically the various phases of high- $p_T$  photon studies. The large solid-angle layout (Phase I) has been used for the measurement of very high  $p_T \pi^0$ 's,  $e^+e^-$  pairs, and single photons up to  $p_T \sim 3 \text{ GeV}/c$ . Single-photon data obtained with layout II are discussed here. A recent run (layout III) aimed at the independent verification of the result of II.

effects. The high spatial segmentation achievable with the liquid-argon ion chamber technique resulted in a spatial resolution of typically  $\sigma \sim 5$  mm and allowed us to separate the two photons from symmetric  $\pi^0$  decays, up to  $\sim 10$  GeV/c depending on the experimental layout. The fourfold longitudinal subdivision allowed effective hadron-photon discrimination already at the triggering stage.

As emphasized in the Introduction, the success of this photon identification method has to be based on two requirements:

- identification of the single photons and discrimination against hadrons through detailed study of the longitudinal and transverse shower distribution in the calorimeter;
- discrimination against photons originating from decays of  $\pi^0$ 's,  $\eta$ 's,  $\eta'$ 's,  $\omega$ 's, etc. This imposes two contradictory constraints on the experimental apparatus: identification of near-by showers from  $\pi^0$  decay requires the highest achievable spatial resolution; on the other hand, the background from very asymmetric decays has to be minimized by using detectors of adequate geometrical acceptance.

Details of the data selection are given in Table 3. The evaluation of the efficiency of these requirements was based on measurements (in test beams and at the ISR) and on computer simulations of the performance of the apparatus<sup>7</sup>). Note that the selection of photons or  $\pi^0$ 's unaccompanied by any additional photon or charged particle within the solid angle covered by one calorimeter module introduces a physics bias: the yield of  $\gamma$ 's and  $\pi^0$ 's measured under these experimental conditions is not truly inclusive.

Table 3  
Selection requirements on data

Requirement	Comment
Triggering	Localized energy deposit consistent with electromagnetic shower development; trigger efficiency measured to be $0.95 \pm 0.05$ for photons with $E_\gamma > 3$ GeV and $0.7 \pm 0.05$ for $\pi^0$ 's with $E_{\pi^0} > 3$ GeV.
Off-line reconstruction of photons	Calorimeter provides four independent views allowing stereo reconstruction of showers; a minimum of 200 MeV energy deposit is demanded per view; consistency of longitudinal and transverse energy deposit with electromagnetic shower is required.
"Unassigned" energy less than 35 MeV	Unassigned energy corresponds to total energy deposit in the front sections of the calorimeter, which is not reconstructed as a shower. Eliminates e.g. accompanying hadrons.
Fiducial area, $0.3 \text{ m} \times 1.2 \text{ m}$ concentric with active calorimeter area of $0.56 \text{ m} \times 1.5 \text{ m}$	For single $\gamma$ : only one shower in fiducial volume and no shower in veto area. For $\pi^0$ (or $\eta$ ): two showers inside fiducial volume, reconstructing to give a consistent mass value, and no shower in veto area.

The measured  $\gamma/\pi^0$  ratio has to be corrected for two trivial sources of apparent single photons: asymmetric decay of mesons ( $\pi^0$ ,  $\eta$ ,  $\eta'$ ,  $\omega$ ) will result in topologies where one photon satisfies all criteria and the other one misses the detector completely. The correction is based on the meson yields measured in the same apparatus<sup>8</sup>) and on Monte Carlo

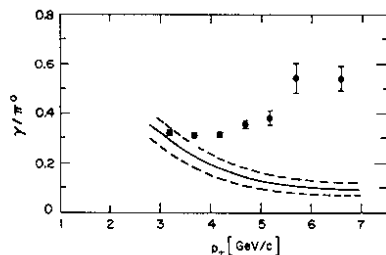


Fig. 4 Observed ratio of  $\gamma$  to  $\pi^0$  for data from all energies. The error bars give statistical errors only. The smooth line indicates the Monte Carlo prediction for the ratio assuming no direct  $\gamma$  production. The dashed lines indicate the one standard deviation systematic errors on the Monte Carlo simulation.

evaluation of the specific experimental conditions. Also, the two photons from  $\pi^0$  decay may be close enough to appear "merged" after shower reconstruction. These results of the Monte Carlo calculation are summarized in Fig. 4, showing the apparent  $\gamma/\pi^0$  ratio. This has to be compared (Fig. 4) with the observed yield, showing a net excess which rises from approximately 0% to about 25% at the highest transverse momentum.

#### 4. DISCUSSION OF RESULTS

##### 4.1 Background

Several other sources may produce an apparent excess of single showers.

The level of hadron background is estimated from a test beam exposure of the calorimeter to hadrons and electrons. Applying the same data selection criteria as that used in the  $\gamma$  analysis, we obtain

$$\frac{\text{acceptance of a } \pi^-}{\text{acceptance of a } e^-} \approx 0.4\% .$$

Assuming pessimistically that other hadrons are equally likely to simulate a photon, we arrive at an upper limit on the hadron background of  $\leq 2\%$ .

Cosmic rays or beam-gas interactions may also be confused with single photons. The effect of this background was estimated to be below 2% of the observed  $\gamma/\pi^0$  ratio.

A non-linear energy response of the calorimeter, rising faster than linear with incident photon energy, would contribute to the  $\gamma/\pi^0$  ratio. Information on the energy response of our calorimeter modules is shown in Fig. 5 together with the level of non-linearity, which would be required to reproduce our measurements with this effect alone. The effect of a non-linearity has been included in the systematic errors.

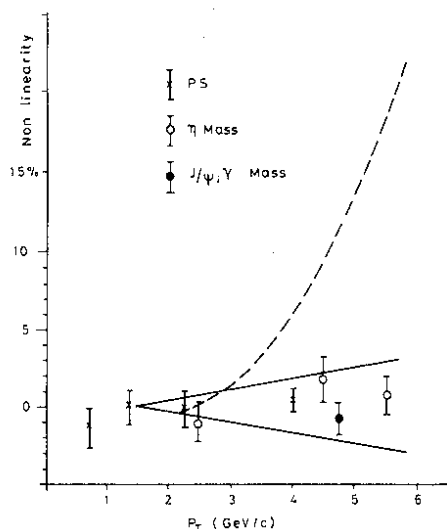


Fig. 5 Differential energy linearity of the liquid-argon calorimeter. Crosses are from an exposure to a momentum-analysed electron beam. Open circles are obtained from the reconstruction of  $\eta \rightarrow \gamma\gamma$  events over the interval  $1.5 < p_T < 8$  GeV/c. The closed circle is based on a comparison of the  $J/\psi$  and  $\Upsilon$  masses. Also shown is the required non-linearity if this effect alone were to explain the measured  $\gamma/\pi^0$  ratio (dashed line). Systematic errors given in the text are based on the non-linearity shown by the solid lines.



#### 4.2 Summary of experimental results

In Fig. 6 we show the results obtained with set-up II at three  $\sqrt{s}$  values. Error bars shown include both systematic and statistical errors. The results are consistent with preliminary data of a recent run (set-up III), where some of the critical experimental parameters, such as the effective solid angle, were changed. This indicates, for example, that the physics bias of some of the previously described cuts does not affect the data in a drastic way. For comparison, we also show (Fig. 7) three different theoretical curves, estimated for the *inclusive* ratio  $\gamma/\pi^0$ . Besides the subprocesses mentioned earlier, the prediction of Rückl et al.<sup>2)</sup> assumes also different CIM mechanisms, estimated to contribute particularly at the intermediate  $p_T$  values.

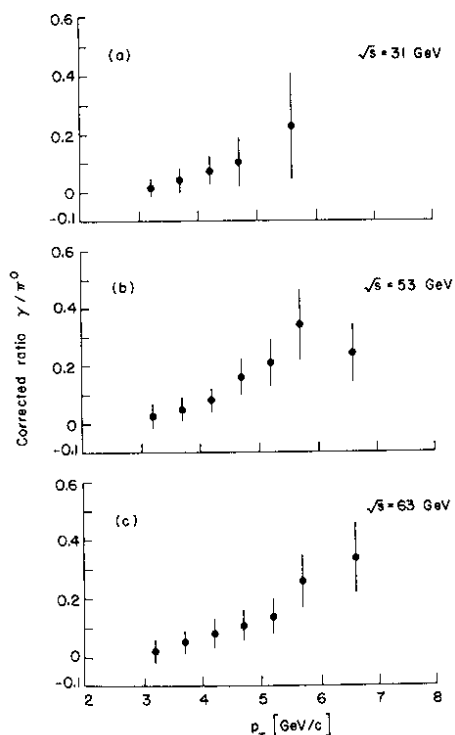


Fig. 6 The measured  $\gamma/\pi^0$  ratio at three  $\sqrt{s}$  values after subtraction of all sources of apparent  $\gamma$  production.

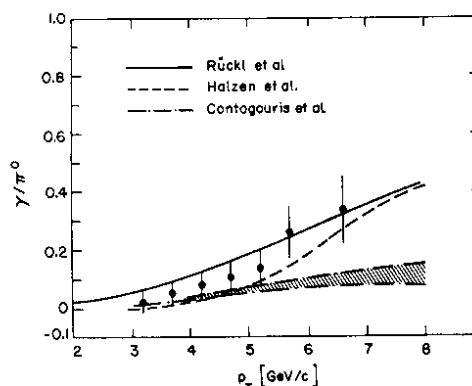


Fig. 7 The measured  $\gamma/\pi^0$  ratio ( $\sqrt{s} = 63$  GeV) and comparison with three different theoretical estimates. The calculation of Contogouris et al. was carried out for  $\sqrt{s} = 52$  GeV and for two different sets of structure functions (shaded area).

Also shown is a calculation [Contogouris et al.<sup>9)</sup>] where scale-breaking effects were explicitly included in the treatment, resulting in a rather strong suppression at large transverse momenta.

Some information on direct  $\gamma$  production is available from other groups and is summarized in Figs. 8 and 9. The data of the CERN-Rome-BNL Collaboration<sup>10)</sup> show, within very large errors, the trend of an increasing  $\gamma/\pi^0$  ratio, not inconsistent with our measurements. Data of the FNAL-Johns Hopkins Group<sup>11)</sup> also show a similar  $p_T$  dependence. Note the rather substantial value for  $\gamma/\pi^0$  at 2 GeV/c, which may perhaps be explained by the rather large  $x_{||}$  acceptance of this experiment. Another experiment at the ISR, using the "external converter method", reports an upper limit of  $\gamma/\pi^0 \leq 30\%$  at  $p_T = 10$  GeV/c<sup>12)</sup>.

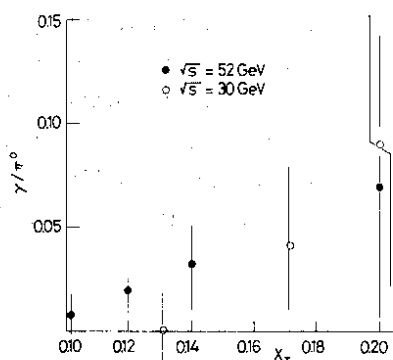


Fig. 8 Results on  $\gamma/\pi^0$  obtained by the CERN-Rome-BNL Collaboration at the CERN ISR.

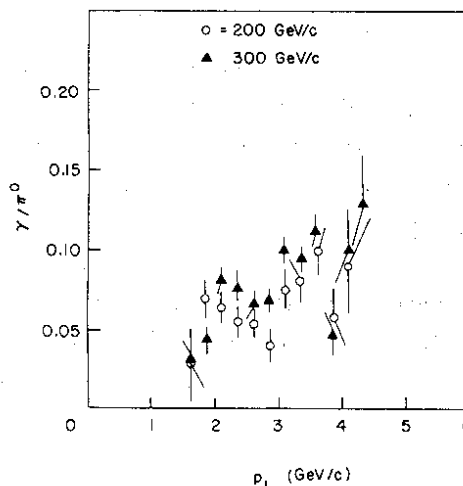


Fig. 9 Preliminary results of the FNAL-Johns-Hopkins Group on  $\gamma/\pi^0$  production.

### 5. CONCLUSIONS

We have presented experimental evidence for direct production of photons in pp collisions. The ratio  $\gamma/\pi^0$  rises from below  $\sim 1 \pm 1\%$  at  $p_T \approx 2.5$  GeV/c to about  $25 \pm 8\%$  at  $p_T \approx 7$  GeV/c. The  $p_T$  dependence of this ratio is consistent with the production level predicted by QCD. The very large  $p_T$  regime (up to and beyond 10 GeV/c), where scale-breaking effects are expected to be observable, remains to be explored. The study of direct photon production should be developed into a probe of the gluon distribution: this requires experiments combining the measurement of the complete event structure together with excellent photon identification capabilities.

### REFERENCES

- 1) G.R. Farrar, Phys. Lett. 67B, 337 (1977).
- 2) We mention, in particular, the results of two groups, which have been used in comparison with our data:  
R. Rückl, S.J. Brodsky and J.F. Gunion, Phys. Rev. D 18, 2469 (1979).  
F. Halzen and D.M. Scott, COO-881-21 (1978).
- 3) J.H. Cobb et al., Phys. Lett. 78B, 519 (1978).
- 4) G.R. Farrar and S.C. Frautschi, Phys. Rev. Lett. 36, 1017 (1976).
- 5) A. Chilingarov et al., Contribution submitted to the 19th Int. Conf. on High-Energy Physics, Tokyo, 1978.
- 6) J.H. Cobb et al., Nucl. Instrum. & Methods 158, 93 (1979).
- 7) The Monte Carlo program of the electromagnetic cascade is described in: R.L. Ford and W.R. Nelson, SLAC-210 (1978).
- 8) C. Kourkouvelis et al., Phys. Lett. 84B, 270 and 277 (1979).  
C. Kourkouvelis et al., Inclusive  $n'$  and  $\omega$  production at the CERN ISR, in preparation.
- 9) A. Contogouris et al., Phys. Rev. D 19, 2607 (1979).
- 10) E. Amaldi et al., Phys. Lett. 84B, 360 (1979).
- 11) B. Fox, private communication.
- 12) A.L.S. Angelis et al., Phys. Lett. 79B, 505 (1978).